# Experimental Analysis of Multiple Scattering BRDF Models

Feng Xie*
Stanford University
Facebook Reality Labs
USA
feng.xie@fb.com

James Bieron*
College of William & Mary
USA
jcbieron@email.wm.edu

Pat Hanrahan
Stanford University
USA
hanrahan@cs.stanford.edu

Pieter Peers
College of William & Mary
USA
ppeers@siggraph.org

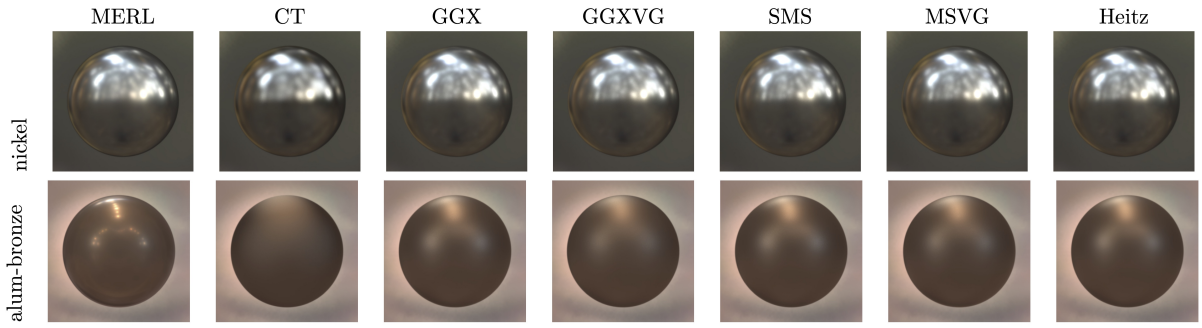


**Figure 1: Comparing measured MERL BRDFs with adaptively fitted microfacet BRDF models (Cook Torrance, GGX, GGX with V-Groove shadowing term, GGX with approximate multiple-scattering, GGX with V-Groove based multiple scattering, and GGX with Smith based multiple scattering) under 2 different lighting environments.**

## CCS CONCEPTS

• **Computing methodologies** → **Reflectance modeling**; **Rendering**.

## KEYWORDS

Appearance Modeling, Microfacet Models, Multiple Scattering

**ACM Reference Format:**
Feng Xie, James Bieron, Pat Hanrahan, and Pieter Peers. 2021. Experimental Analysis of Multiple Scattering BRDF Models. In *SIGGRAPH Asia 2021 Technical Communications (SA '21 Technical Communications), December 14–17, 2021, Tokyo, Japan.* ACM, New York, NY, USA, 4 pages. https://doi.org/10.1145/3478512.3488601

## 1 INTRODUCTION

Microfacet-based reflection models are widely used in visual effects applications ranging from computer games to animation and feature film rendering. However, standard microfacet BRDF models do not account for light transport that scatters more than once on a rough surface, which can lead to significant energy loss. As physically based rendering becomes more prevalent in production applications, this lack of energy preservation becomes problematic. To preserve energy, a number of multiple scattering BRDF models have been introduced. Heitz et al. [2016] leverage a volumetric approach for modeling multiple scattering accurately, but its stochastic evaluation results in increased variance. Xie and Hanrahan [2018] and Lee et al. [2018] introduced an efficient analytical multiple scattering model, albeit with a singularity in the direction of mirror reflection. Turquin [2019] build on the work of Kula et al. [2017] and derive an efficient to evaluate and importance sample, albeit approximate, multiple scattering model. While these multiple scattering BRDF models are based on sound theoretical foundations (i.e, energy preservation and color saturation in rough metals due to multiple scattering), their practical relevance for modeling real world materials is unknown.

In this paper, inspired by Ngan et al.'s [2005] experimental analysis of 7 single scattering BRDF models, we present the first comprehensive experimental analysis of multiple scattering BRDF models, using both a traditional cosine weighted L2 BRDF fitting metric as well as an image based adaptive metric [Bieron and Peers 2020] on the MERL material database [Matusik et al. 2003] (Figure 1). We show that, although physically based multiple scattering BRDF models slightly reduce fitting errors for rough materials, the perceptual visual difference between multiple scattering BRDF models and a standard GGX BRDF model is negligible for the majority of measured materials. Our experiments show that a blend of a Lambertian and a GGX lobe can fit most of the rough MERL materials well, except for a few materials that exhibit phenomena beyond the capabilities of a microfacet BRDF model (with or without multiple scattering), such as inter-fiber scattering (in fabrics), or complex subsurface scattering in between the top coating layer and the diffuse substrate.

*Joint first authors.


*SA '21 Technical Communications, December 14–17, 2021, Tokyo, Japan*

ACM ISBN 978-1-4503-9073-6/21/12…$15.00
https://doi.org/10.1145/3478512.3488601

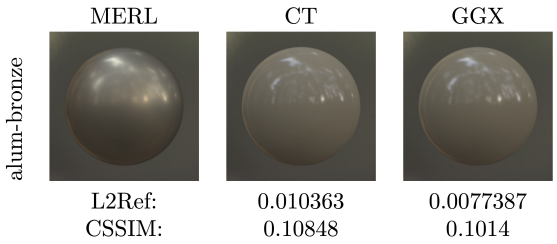


**Figure 2: An example of cosine weighted L2 BRDF fitting overestimating the diffuse component.**

## 2 METHODOLOGY

Similar to Ngan et al. [2005], we perform our experimental analysis on the MERL material database [Matusik et al. 2003] of 100 isotropic measured BRDFs.

### 2.1 Microfacet Models with Multiple Scattering

We perform our experimental analysis on 3 GGX-based extensions designed to model multiple scattering effects: a microflake-based multiple scattering for GGX with the Smith shadowing term presented by [Heitz et al. 2016] (denoted by *Heitz*); a multiple scattering model for GGX with a V-groove based shadowing term [Xie and Hanrahan 2018] (*MSVG*); and a compute efficient approximate multiple scattering model for GGX [Turquin 2019] (*GGXSMS*). To serve as a baseline, we include 3 single scattering BRDF models: the single scattering GGX BRDF model with the Smith shadowing term [Walter et al. 2007] (*GGX*); the GGX BRDF with a V-groove based shadowing term (*GGXVG*); and the classic Cook-Torrance BRDF with the Smith shadowing term (*CT*).

.

### 2.2 Parametric Fitting

We follow common practice and use a composite BRDF $f$ consisting of a Lambertian diffuse lobe and a specular lobe chosen from the above set of microfacet reflection lobes. Since our specular models have the same 5 input parameters, all composite BRDF models have 8 parameters: diffuse albedo, specular albedo, roughness ($\alpha$), and the index of refraction ($\eta$).

We quantify a BRDF model's ability to represent a real world material $M$ as the minimal fitting error achieved by any set of parameters $p$ for the BRDF $f$ compared to the measured values of $M$. Finding the set of minimizing parameters $p$ typically requires a non-linear optimization: $\text{argmin}_p\, E(f(p), M)$, where $E$ is an appropriate error/fitting metric. Additional constraints can be added to enforce physical plausibility of the fitted parameters such as energy conservation. However, in this paper we do not add such constraints, and focus our investigation on the raw ability of the model to represent the measured data.

### 2.3 Fitting Metric

The most common error/fitting metric is the cosine weighted $L2$ measure, and which was also used in Ngan et al.'s [2005] experimental analysis. However, minimizing this error measure typically does not lead to a good visual match when comparing renderings of the fitted BRDF and measured BRDF under some target lighting. This mismatch is especially prevalent for measured materials with strong specular peaks that tend to dominate the fitting error, and as a consequence over or under estimate the diffuse term (Figure 2).

To strike a balance between data fidelity and visual fidelity, Bieron and Peers [2020] presented a two stage, image based adaptive fitting metric: in the first stage data fidelity is maximized according to a set of generalized error metrics $E_\gamma$, yielding a set of candidate fits $f_\gamma$ for each measured material $M$:

$$\sum_{\theta_i,\theta_o,\phi_d} w(\theta_i,\theta_o)([f_\gamma(\omega_i,\omega_o)cos\theta_i)]^{\frac{1}{\gamma}} - [M(\omega_i,\omega_o)cos\theta_i)]^{\frac{1}{\gamma}})^2, \tag{1}$$

where $\gamma \in [1,3]$ and $w = \sin\theta_i \sin\theta_o \cos\theta_o$ [1]. Note when $\gamma = 1$, equation 1 is the same as the cosine weighted $L2$ metric. In the second stage, an image based metric (CSSIM or LPIPS) is used to select among $\{f_\gamma\}$, the BRDF fit with the best visual match on a set scene for a given material $M$ (i.e., a sphere lit by the *Eucalyptus Grove* light probe).

We perform our experimental analysis of multiple scattering BRDF models using both error metrics: the cosine weight $L2$ error as well as the adaptive image based metric using CSSIM.

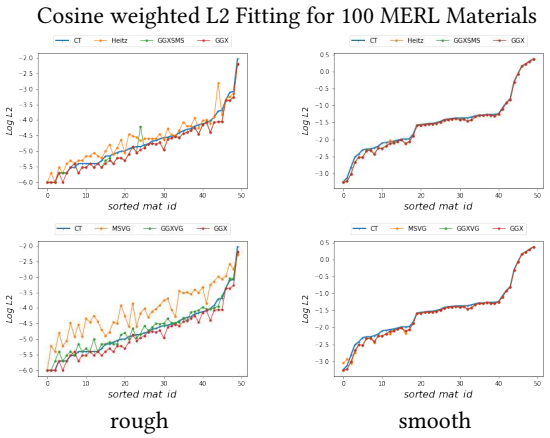


**Figure 3: Cosine weighted L2 error for the different BRDF models sorted by the error on the Cook-Torrance model.**

## 3 ANALYSIS OF FITTING RESULTS

We present error graphs for the cosine weighted $L2$ fitting and CSSIM based adaptive fitting in Figures 3 and 4 respectively.

To simplify our analysis, we split the 100 MERL materials in two equal groups of 50 materials that roughly correspond to *smooth* and *rough* materials. The classification is done using the median roughness $\alpha$ of the Cook-Torrance (*CT*) BRDF fits.

To improve visual clarity in the error plots, we divide the 6 models into 2 groups of 4, using the *GGX* and *CT* models as baseline anchors across the two groups. Since the *CT* model has the largest error range for both $L2$ and adaptive fits, all materials are sorted in order of the *CT* fitting error in all graphs.

[1]The term $\sin\theta_i$ is the Jacobian of $(\phi_i,\theta_i)$ with respect to solid angle, and the term $\sin\theta_o \cos\theta_o$ is the Jacobian for the projection of the visible hemisphere of outgoing directions $(\phi_o,\theta_o)$ to a disc [Bieron and Peers 2020].

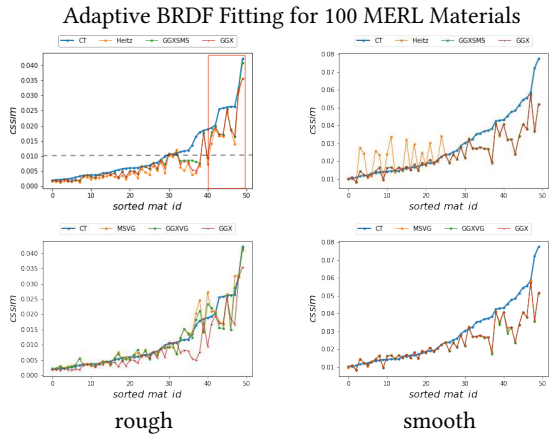


**Figure 4: CSSIM error for each model fitted with the adaptive image-based BRDF fits.**

*Single Scattering BRDF Models.* For smooth materials, we observe for classic *single scattering* BRDF models (*CT*, *GGX*, and *GGXVG*) that there is little difference in terms of data fidelity (Figure 3, right-bottom). However, there is more difference in the models' ability to visually match the materials, and the choice of the microfacet distribution dominates the CSSIM error (Figure 4, right-bottom). Unsurprisingly, we see that the GGX distribution is much better than the Beckmann distribution in replicating the specular appearance of real materials. For rough materials, we observe that the shadowing and masking term impacts the data fidelity for *single scattering* BRDF models (Figure 3, left-bottom, green-curve vs blue/red curve) as well as visual fidelity (Figure 4, left-bottom). In both cases, we observe that the V-groove based shadowing and masking term is less effective than the Smith shadowing and masking term.

*Multiple Scattering BRDF Models.* Multiple scattering BRDF models (*Heitz, MSVG, GGXSMS*) are designed to account the scattering of light, most prominent in rough materials. For smooth materials, we expect that multiple scattering plays a much smaller role. This expectation is validated by the fitting results shown in the error plots on the right side of Figures 3 and 4, where all three multiple scattering BRDF models have almost identical *L2* fitting error and adaptive fitting error as the standard GGX model. A notable exception is the Heitz BRDF model, which shows a higher CSSIM error for a number of smooth materials. This increased CSSIM error is likely due to the stochastic nature of the Heitz BRDF model which can lead to higher variance (even though we use $8k$ samples per pixel for image generation).

For the 50 rough materials, we observe notable, and unexpected, differences between the error curves for the *MSVG* and *Heitz* models compared to the *GGXVG* and *GGX* BRDF models. First, the *MSVG* model yields a lower data fidelity (i.e., higher *L2* fitting error) compared to all the other BRDF models (Figure 3 left-bottom). We conjecture that this is due to the singularity in the *MSVG* model's multiple scattering lobe, causing an overestimation of the BRDF's diffuse term to compensate for the error in the specular term as illustrated in Figure 5. A second notable difference is that the stochastic nature of the *Heitz* model causes it to exhibit a generally

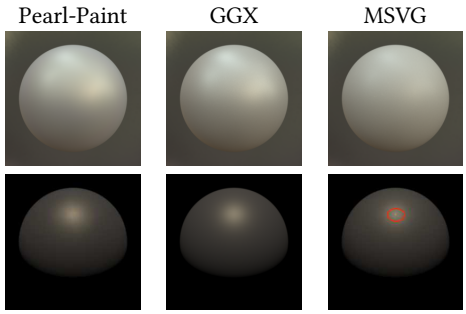


**Figure 5: The *MSVG* model results in a too diffuse fit (top row) for the *Pearl-paint* material due to the model's singularity in the reflected direction, visible under directional lighting (bottom row).**

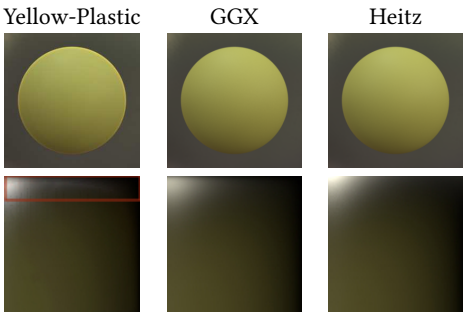


**Figure 6: BRDF slices at $\phi_d = 90°$ show that the fitted *GGX* and *Heitz* BRDFs for the *Yellow-Plastic* material are missing the Fresnel peak present in the measured BRDF (bottom row), resulting in the yellow rim highlight to be missing from the rendered images (top row).**

higher *L2* error than the *GGX* and *CT* BRDF models (Figure 3 left-top). However, the *Heitz* model's adaptive image error is generally lower (Figure 4 left-top). Furthermore, the CSSIM errors of the *Heitz* models fitted using the *cosine weighted L2* metric also shows similar or better visual fidelity compared to the standard *GGX* model [2]. However, the visual improvement is subtle for the vast majority of the rough materials, mainly due to two reasons: *Multiple scattering transport is not the main source of fitting errors* and *visual similarity of single scattered and multiple scattered reflectance.*

*Multiple scattered Transport is not the Main Source of Fitting Errors.* We focus our investigation on the top 10 rough materials with the worst visual errors when using the *GGX* model (those with CSSIM greater than 0.01) and observe little difference in visual errors between *GGX* and *Heitz* models (the red box enclosed region in Figure 4 left-top). For these materials we observe that there are two main types of fitting errors:

- *Poor fitting of the specular highlight.* Metals in MERL dataset often show a soft specular fall off in addition to an intense specular peak. This dual specular lobe appearance falls outside the representative space of what can be modeled by a

[2]This error graph is provided in the supplementary report

**Figure 7: The Utah Teapot under environment lighting with *GGX* and *Heitz* BRDF models using their fitted parameters for *Alum-Bronze* and difference($x2$) images (left to right): $|Heitz(p_{Heitz}) - GGX(p_{GGX})| * 2$, $GGX(p_{GGX})$, $Heitz(p_{Heitz})$, $GGX(p_{Heitz})$, and $|Heitz(p_{Heitz}) - GGX(p_{Heitz})| * 2$.**

single GGX lobe. Heitz et al. [2016] showed that the multiple scattering lobe looks like a scaled-down version of the single scattering lobe. As a consequence, these multiple scattering models also cannot model this second soft specular fall off.

- *Poor fitting of grazing reflections.* Burley [2012] noted that the grazing reflectance behavior includes Fresnel and grazing retro-reflection in rough material in the MERL dataset due to subsurface scattering and fiber scattering. These effects can not be modeled by the linear combination of a Lambertian and a microfacet model, as shown in Figure 6 where we compare cosine weighted $\phi_d = 90^\circ$ slices of the *Yellow-Plastic* material (i.e., one of the worst fitted rough materials) fitted with the *GGX* and *Heitz* BRDF models. While the *Heitz* model exhibits a brighter grazing specular peak in the slice image, the yellow highlight stripe near the Fresnel peak is missing for both models.

*Visual Similarity of Single Scattered and Multiple Scattered Reflectance.* Due to the inclusion of multiple scattering, rendering the *Heitz* model using the same parameters as the *GGX* BRDF for a rough material would result in a brighter image as more energy is preserved (right most image in Figure 7 shows the difference between the *Heitz* and *GGX* models using fitted parameters from the *Heitz* model for *Aluminum-Bronze*). Yet, the visual differences between the fitted *Heitz* and *GGX* BRDF models are barely visible for the majority of the rough MERL materials (left most image in Figure 7 shows the difference between the fitted *Heitz* and *GGX* models for *Aluminum-Bronze*), because the fitting procedures compensate by increasing the specular albedo and roughness for the standard *GGX* model. We show in our supplementary report that for most of the rough materials, the specular albedo and roughness $\alpha$ for the *GGX* model fits are higher than the corresponding parameters in the *Heitz* BRDF fits. [3]

From the above observation we can conclude that even though the standard *GGX* microfacet BRDF model loses energy for rough materials, it is possible to compute an appropriate $albedo'$ and $\alpha'$ such that $GGX(albedo', \alpha')$ closely matches the behavior of $Heitz(albedo, \alpha)$; see Figure 7. While our experiments confirm that the *Heitz* BRDF model is an accurate model of multiple scattering reflection effects on rough surfaces, it is expensive to compute and its stochastic nature often requires $8x$ samples for convergence. Instead, computing an adaptive image based fit of a *GGX* BRDF to match the appearance of the *Heitz* model, means we can approximate the effects of multiple scattering efficiently and accurately in real time applications as well as physically based rendering systems without the computational overhead of the *Heitz* model.

[3] We scaled the difference images in Figure 7 by 2x to make them more visible.

## 4 SUMMARY

We provide an experimental confirmation of prior observations by Burley et al. [2012] on single scattering models and Heitz et al. [2016] on multiple scattering through a comprehensive analysis of three single scattering microfacet models and the three GGX-based multiple scattering models using the MERL dataset. In addition, we presented several new insights on the ability and limitations of these models:

- The shape of the microfacet distribution function is most important for smooth materials, as indicated by the dramatic difference in fitting quality difference between the *Cook-Torrance* and *GGX* based models for metals.
- The impact of the shadowing and masking term increases with roughness, as shown by the decrease in fitting quality of the V-groove vs. Smith shadowing and masking term for rough materials vs. smooth materials in the MERL dataset.
- The combination of a Lambertian component and a *GGX* specular lobe can well approximate the appearance of MERL materials without a double specular highlight or strong grazing highlight.
- For most of MERL materials, a regular single scattering *GGX* specular lobe can approximate the appearance of a *Heitz* multiple scattering specular lobe by appropriately adjusted parameters.

In the future, we would like to include physical constraint such as energy conservation and plausible Fresnel values in the fitting procedures and evaluate whether the above conclusions still hold. Furthermore, we would also like to explore using the adaptive fitting method to perform parameter inversion to account for multiple scattering effects in microfacet models.

## ACKNOWLEDGMENTS

James Bieron and Pieter Peers are partially supported by NSF grant IIS-1909028.

## REFERENCES

James C. Bieron and Pieter Peers. 2020. An Adaptive BRDF Fitting Metric. *Computer Graphics Forum* 39, 4 (July 2020).

Eric Heitz, Johannes Hanika, Eugene d'Eon, and Carsten Dachsbacher. 2016. Multiple-scattering Microfacet BSDFs with the Smith Model. *ACM Trans. Graph.* 35, 4, Article 58 (July 2016).

Stephen Hill, Burley Brent McAuley, Martinez Adam Yoshiharu Gotanda, and Naty Hoffman Brian Smits. 2012. Physically Based Shading in Theory and Practice. In *ACM SIGGRAPH 2012 Courses.* Article 7.

Stephen Hill, Stephen McAuley, Alejandro Conty, MichałDrobot, Eric Heitz, Christophe Hery, Christopher Kulla, Jon Lanz, Junyi Ling, Nathan Walster, Feng Xie, Adam Micciulla, and Ryusuke Villemin. 2017. Physically Based Shading in Theory and Practice. In *ACM SIGGRAPH 2017 Courses.* Article 7.

Joo Lee, Adrián Jarabo, Daniel Jeon, Diego Gutiérrez, and Min Kim. 2018. Practical multiple scattering for rough surfaces. *ACM Transactions on Graphics* 37, 1–12.

Wojciech Matusik, Hanspeter Pfister, Matt Brand, and Leonard McMillan. 2003. A Data-Driven Reflectance Model. 22, 3 (2003).

A. Ngan, F. Durand, and W. Matusik. 2005. Experimental Analysis of BRDF Models. *Comp. Graph. Forum* (2005), 117–226.

Emmanual Turquin. 2019. Practical multiple scattering compensation for microfacet models. https://blog.selfshadow.com/publications/turquin/ms_comp_final.pdf

Bruce Walter, Stephen R. Marschner, Hongsong Li, and Kenneth E. Torrance. 2007. Microfacet Models for Refraction Through Rough Surfaces. *Comp. Graph. Forum* (2007), 195–206.

Feng Xie and Pat Hanrahan. 2018. Multiple scattering from distributions of specular V-grooves. *ACM Trans. Graph.* 37, 6 (2018).